

# Thermochromic Detection of Ultrasound-Induced Nanoparticle Heating in Tissue-Mimicking Solid Gel

Huiting Lin

National Chiao Tung University

Nelson Gee-Con Chen (✉ [ngchen@nctu.edu.tw](mailto:ngchen@nctu.edu.tw))

National Chiao Tung University <https://orcid.org/0000-0002-9843-2922>

Chih-Mao Huang

National Chiao Tung University

---

## Research

**Keywords:** nanoparticle, temperature sensor, ultrasound heating

**Posted Date:** May 19th, 2020

**DOI:** <https://doi.org/10.21203/rs.3.rs-28383/v1>

**License:** © ⓘ This work is licensed under a Creative Commons Attribution 4.0 International License.

[Read Full License](#)

---

# Abstract

## Background

Microbubble has been extensively used for ultrasound imaging and many other applications such as ultrasound cleaning. Few studies have been reported on ultrasound interactions with small nanoparticles (< 250 nm). Due to the broad use of nanoparticles in many different fields, it is critically important to clarify whether nanoparticles can have strong interaction with ultrasound. In addition, Nanoparticle assisted ultrasound therapy has recently been found to have selective killing of cancer cells compared to normal cells. Nevertheless, the mechanism is not known. The major possible mechanisms for killing cells are cavitation and heating. In this work, a simple thermochromic method is developed to clearly indicate that the interaction of nanoparticle with ultrasound can lead to temperature rise that can lead to selective killing of cancer cells.

## Results

Direct three-dimensional detection of ultrasonically induced heating in a nanoparticle bearing tissue-mimicking gel would provide a means to estimate their effectiveness as thermally-based sonosensitizers. Such a gel was produced through the addition of an irreversible thermochromic liquid to a well-known agarose gel during fabrication. Polystyrene nanoparticles were embedded within gels during production. The placement of gels within a temperature-controlled bath set to a temperature below the transition temperature allows for the visual detection of slight temperature increases. The modified gel material was shown to undergo color change upon heating to 54 °C from blue to white. The appearance of white color on the gel is a clear indication of nanoparticle to enhance the ultrasound energy to increase the temperature of gel. Nanoparticle presence within a solid causing increased heating upon ultrasound exposure, as detected through thermochromicity, is reported for the first time.

## Conclusion

Even small nanoparticles can have significant interaction with ultrasound to lead to temperature rise in the medium. Therefore, the selective killing of cancer cells more than normal cell should be primarily from heating instead of cavitation since cancer cells in general cannot survive in higher temperature than normal cells. Cavitation should lead to the killing of both cancer and normal cells due to the release of a large amount of energy in the process. Direct three-dimensional detection of ultrasonically induced heating in a nanoparticle bearing tissue-mimicking gel becomes feasible.

## Background:

This work was initially motivated by one of our recent studies in which nanoparticle presence was shown to increase the effect of ultrasound on biological specimens. Ultrasound with nanoparticles was shown

to be more effective at destroying cultured cancerous cells relative to normal ones (Nanoparticle-Assisted Ultrasound Therapy (NAUT)) [1]. In mice, implanted tumors were more effectively shrunk with ultrasonic exposure with nanoparticle injection into the circulation relative to controls [2]. Similarly, mice that received intra-tumoral injections of nanoparticles prior to ultrasound exposure had their tumors raised to temperatures, based on thermometer-type measurements, higher than those receiving sham injections [3]. Magnetite nanoparticle agglomerates were shown to allow high-intensity focused ultrasound to destroy tumor spheroids, relative to controls with no agglomerates, with the cause attributed to increased inertial cavitation [4].

Contrast agents such as perfluorocarbon microparticles have been broadly used for ultrasound imaging and drug delivery [5]. The enhancement of the contrast agent depends on backscattering, beam attenuation, and difference in speed of the sound. Particle size and material are two key factors for being a good contrast agent. Nevertheless, microbubble contrast agents are limited by the stability and the large size to get through small blood vessel especially the vessels in the tumors are typically between 380 nm and 780 nm [6]. In general, the scattering cross-section for a single bubble,  $\sigma$ , is proportional to the sixth power of the radius. Small nanoparticles are not in favor for enhancement. Reduction in diameter by a factor of 10 could lower the cross section by six orders of magnitude. Furthermore, the bubble resonance frequency is inversely proportional to the size; this would require very high frequency transducers. Nevertheless, nanoparticle, in principle can be a better ultrasound contrast material due to the impedance mismatch between solid and soft tissue. [7] Nanobubble and nanodroplet as contrast have been pursued with most works at several hundred nanometer region. In HIFU (high-intensity focused ultrasound), magnetic nanoparticle presence reduces the required time and power needed to generate a given lesion [8]. Nanoparticles are a form of sonosensitizer, which are defined as something which concentrates ultrasonic effects where they are located. Few works on smaller nanoparticles with ultrasound have been studied. In this work, we give a clear evidence that solid nanoparticles in the gel to be irradiated with ultrasound can clearly lead to the temperature increase. This rise of temperature can cause the selective killing of cancer cells than its counter normal cells.

Polystyrene nanoparticles have been used extensively to study characteristics and functions of cells and cell membranes. For instance, their interactions with hepatocytes and hepatocyte cell lines [9], ovarian cancer cells [10], astrocytoma cells [11], kidney epithelial cells [12–13], fibroblasts [12–14], gastric adenocarcinoma [15], neurons and microglial cells [16], as well as colon [17] and lung [18] cancer cell lines have already been reported. Nanoparticles suspended in liquid cause the liquid temperature rise upon insonation to be greater than that of particle-free controls [21–23]. In tissue-mimicking phantoms, nanoparticle presence caused increased heating with ultrasound, and the increased heating is different depending on the nanoparticles used [21–22]. To date, only a couple of measurements have been pursued. Nearly all of them obtained temperature by using embedded thermocouples, which are limited to measuring temperatures at specific locations. In addition, they are subject to measurement artifact caused by their presence [24]. One exception to such is the study [24] by Józefczak and colleagues, which used an infrared camera to record temperature rises in agar phantoms with embedded magnetic

nanoparticles. This approach, however, is limited to examining temperatures reached at the phantom surface. Temperatures in the phantom interior cannot be measured using this approach.

The agarose-based tissue mimicking gel is the most commonly used ultrasound imaging phantom material [25]. It was developed by Madsen and colleagues [26], and provides a platform for all sorts of ultrasonic studies. These studies include imaging system accuracy [27], nonlinear propagation in histotripsy [28], and thermocouple-based measurements of heating arising from a focused ultrasound transducer [29]. Its properties resemble those of soft tissue, and therefore provide a simple platform on which to conduct ultrasonic studies. Thermochromicity is a property specific to some materials in which the material changes color upon changes in temperature. A material can be one particular color over a temperature range, and once outside that range, change to a different color. It can be reversible or irreversible; a reversible material reverts to its original color upon being placed back within its original temperature range, while an irreversible material maintains its new color regardless of subsequent temperature changes.

A pioneering use of thermochromic materials to measure physiotherapy ultrasound fields was performed circa 1997 [30]. Recently reported thermochromic phantoms include those based on polyacrylamide, with one formulation that changes color from blue to colorless upon heating [31] and another that changes color from white to magenta [32–33]. An older formula, based on the addition of bovine serum albumin (BSA) and pH control, produces a phantom with transition temperature ranging from 50–60 °C [34]. Silicone phantoms have also been made to be thermochromic [35]. Two unusual phantom types have been produced that can indicate temperature ranges rather than a simple binary indication of being above or below the transition temperature, with the material by Iwahashi and colleagues [36] being reversible and that by Kim and colleagues [37] being irreversible. These phantom types have not been, to date, applied toward nanoparticle presence and their related additional heating. To obtain temperatures in thermochromic phantom interiors, one would section an irreversible phantom post-exposure. In this work, we report the detection of increased ultrasonic heating of nanoparticle-bearing tissue-mimicking gel with embedded nanoparticles using a thermochromic gel phantom material. Being able to estimate the entire altered temperature field when nanoparticles are present is useful in evaluating the effectiveness of the particles present as thermally based sonosensitizers. Issues with thermocouples are avoided, and a complete three-dimensional map of the ultrasonic field's heating effects can be obtainable with a single ultrasonic exposure.

## **Results:**

### **A. Results of Gel Heating**

Heating of the gel to a temperature of 54 °C caused it to undergo an irreversible color change from blue to white as seen in Fig. 1.

### **B. Effect of Ultrasonic Exposure**

Lesions were most apparent on the bottom side of ultrasound exposed gels; in other words, they were on the side farthest from the transducer face. Representative post-ultrasound gel images are provided in Fig. 2.

Analysis of white area sizes of the experimental samples versus those of the control samples indicates significant differences caused by nanoparticle presence, as shown in Fig. 3. Added nanoparticles caused areas to display additional heating for both nanoparticle sizes examined.

## **Discussion:**

The addition of nanoparticles to suspensions and solids concentrates energy at the nanoparticles. This study indicates that the energy concentration occurs through an increased heating mechanism. Nanoparticle presence causes increases ultrasonic attenuation [39] with concomitant heating [20] as ultrasound travels through the medium. However, the area in which color change is observed should not be taken as the “degree” of heating that occurred. First, detection based on binary color change cannot distinguish between heating to temperatures slightly above the transition temperature, and heating to temperatures substantially above that. Second, while increased attenuation leads to increased heating, total heating even within a given area could be affected by beam propagation effects. Ultrasound underwent multiple reflections with the setup used, which can result in less attenuating areas receiving more energy due to ultrasound passing more times through the area than a corresponding more attenuating area. For beam geometry measurements, one should use a large volume gel block that encompasses the ultrasound beam. Nevertheless, the fact that certain nanoparticle-containing gels had white areas significantly larger than nanoparticle-free controls indicates that their presence caused heating that otherwise would be absent.

The addition of different thermochromic liquids, either alone or in combination, would allow this gel to have different color transition temperatures. A liquid that transitions at a lower temperature than that used may be helpful in mapping the extent of hyperthermia fields, where tissue temperatures are raised to temperatures around 40–46 °C [20]. Since the material solidifies around 37 °C, careful temperature control is necessary in order to add the liquid to the material before the material solidifies; yet the material must also be at a temperature below the lower transition temperature. Thermochromic liquids in combination would combine colors depending on the temperatures reached. The use of irreversible liquids is recommended because they provide permanent changes that can be observed over time. A reversible liquid would revert once the heating ceased, thereby confining measurements and observations to the duration of active insonation.

## **Conclusion:**

Our report is the first of ultrasonic nanoparticle heating detection through the use of a thermochromic gel. Detection through thermochromicity can allow for the three-dimensional mapping of heating volumes, and avoids artifacts caused by thermocouple presence. This detection is achieved through modification

to the agarose tissue-mimicking ultrasonic gel, which undergoes an irreversible transition from blue to white with heating past 54 °C. Polystyrene nanoparticles within the gel cause parts of it to have temperature rises greater than controls upon insonation. The use of a heated bath set to a temperature near the transition temperature meant that slight temperature differences are detectable.

This work gives a good proof that even small nanoparticles can have strong interaction with ultrasound to lead to temperature increase in the surrounding medium. In addition, this work gives the evidence that the temperature increase not cavitation is the primary reason for selective killing of cancer cells compared to its counter normal cells.

## **Methods:**

### **A. Gel Production**

Agarose gels with embedded thermochromic material were produced based on a formula modified from that previously reported [26]. In brief, agarose (Acros Organics medium-low EEO Mr = 0.12, Waltham, Massachusetts, USA), n-propanol, and distilled water were combined and heated to 90 °C in a 1 g: 2 mL: 23 mL ratio until the solid agarose dissolved. Difco laboratory milk powder was used to prepare skim milk (Becton, Dickinson, and Company, Sparks, MD, USA) following manufacturer directions (100 g: 1 L water ratio) and separately heated to 55 °C. The agarose solution was subsequently allowed to cool to 55 °C at which point it was added to the milk in a 7 (agarose solution):5 (milk) ratio by volume. A total volume of 15 mL of the material was extracted, and poured into a separate beaker (height 8 cm, diameter 5.2 cm) preheated to 55 °C. Next, this beaker was allowed to cool to 45 °C, at which point polystyrene nanoparticles (Corpuscular, Cold Spring, New York, USA) and 1.5 mL of a thermochromic liquid (New Prismatic Enterprise Co., LTD., Taipei, Taiwan) that irreversibly changes color upon heating to 54 °C was added. The suspension was stirred thoroughly in order to ensure uniform distribution of all components. With further permitted cooling, it solidified around 37 °C. Experimental samples contained varying numbers and sizes of polystyrene nanoparticles, while control samples did not. Numbers and sizes of nanoparticles examined are detailed in Table I. All experiments were performed in triplicate in order to assess experimental variability.

Table 1  
SIZES AND NUMBERS OF POLYSTYRENE  
NANOPARTICLES EMBEDDED

Size (nm)	Number of Particles / gel
control	0
	$3.3 \times 10^9$
52.4	$6.6 \times 10^9$
	$6.6 \times 10^{12}$
	$5.6 \times 10^7$
204.3	$1.1 \times 10^8$
	$5.6 \times 10^{10}$
	$1.1 \times 10^{11}$

## B. Gel Heating

In order to initially assess the ability of the gel material to change color upon heating, newly cast gel was placed in an ultrasonic cleaner (Elmasonic P 30 H, Elma Schmidbauer GmbH, Singen, Germany). The heating function was used to heat water surrounding the gel to 54 °C. Observations were made of gel appearance at temperatures less than and equal to 54 °C. (At no point was the ultrasonic cleaning function switched on – the ultrasonic cleaner served solely to provide a temperature-controlled water bath.) Photographs were made post temperature exposure, with the gel removed from the bath and allowed to return to room temperature.

## C. Ultrasound Exposure

In order to assess the effect of polystyrene nanoparticle addition to the level of heating caused by ultrasound application, the following setup was used, as illustrated in Fig. 4.

The heated bath feature of an ultrasonic cleaning bath was used to raise the temperature of the gel and its surroundings prior to ultrasonic exposure to 50 °C, which is less than yet near the thermochromic transition temperature. With this arrangement, slight increases in temperature caused by ultrasonic exposure would raise gel temperatures to values above the transition temperature, which would result in visible color changes. Therapeutic ultrasound was applied to the temperature sensitive gels described above using a Sonicator 740 therapeutic ultrasound unit (Mettler Electronics, Anaheim, CA, USA). Sonication parameters were as follows.

- Ultrasonic frequency 3 MHz

- Ultrasonic exposure duration continuous wave (CW) for 10 min
- Mean ultrasonic intensity 1.5 W/cm<sup>2</sup>

The transducer produced a focused bell-shaped cylindrical beam. The maximum beam non-uniformity ratio is 6:1 [38]. The lengthy exposure duration was selected to ensure thermal equilibrium.

## D. Data Analysis

After gels were exposed to ultrasound as described above, they were removed and photographed. Photographs were transferred to ImageJ software (National Institutes of Health, Bethesda, MD, USA). Using that software, white areas were manually estimated by counting the number of bright pixels and converting the pixel numbers to physical areas. These areas were then recorded for each gel. White areas of the control gels were compared with those of the experimental gels using a heteroscedastic (unequal variances) two-tailed Student's T-test (Microsoft Excel, Microsoft Corporation, Redmond, WA, USA). Differences were considered statistically significant at the 0.05 and 0.01 levels.

## Declarations

## Availability of data

The datasets used and/or analysed during the current study are available from the corresponding author on reasonable request.

## Competing interests

The authors declare no competing interests.

## Consent for publication

Not applicable

## Ethics Approval

Not applicable

## Funding

This work was supported in part from a grant (MOST 105-2221-E-009-094) from the Ministry of Science and Technology (MOST) of the Republic of China (Taiwan). (*Corresponding author: Nelson G. Chen.*)

# Author's contributions

HTL performed the experiments, made measurements, and analyzed data. NGC conceived and planned the experimental protocol, performed the data analysis and wrote the manuscript. CMH helped conceive the experimental protocol. All authors read and approved the final manuscript

# Acknowledgements

Not applicable

# References

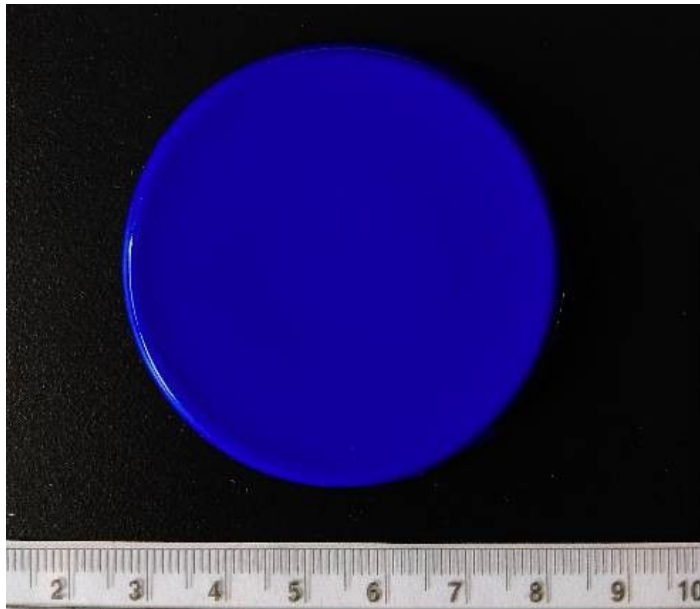
1. Kosheleva OK, Lai TC, Chen NG, Hsiao M, Chen CH. "Selective killing of cancer cells by nanoparticle-assisted ultrasound," *J Nanobiotechnology*, 14, 46, Jun. 2016, 10.1186/s12951-016-0194-9.
2. Kosheleva OK, et al., "Investigation of nanoparticle-assisted ultrasound therapy for treating implanted breast tumors in mice," in *IEEE 17th Intl. Conf. Nanotechnol. (IEEE Nano)*, 2017, pp. 672–674, [Online]. Available: <https://ieeexplore.ieee.org/document/8117465/>.
3. Shakeri-Zadeh A, Khoei S, Khoei S, Sharifi AM, Shiran MB. Combination of ultrasound and newly synthesized magnetic nanocapsules affects the temperature profile of CT26 tumors in BALB/c mice. *J Med Ultrasonics*. Jan. 2015;42(1):9–16. 10.1007/s10396-014-0558-4.
4. Ho VHB, Smith MJ, Slater NKH. Effect of magnetite nanoparticle agglomerates on the destruction of tumor spheroids using high intensity focused ultrasound. *Ultrasound Med Biol*. Jan. 2011;37(1):169–75. 10.1016/j.ultrasmedbio.2010.09.007.
5. Ma YY, Jin KT, Wang SB, Wang HJ, Tong XM, Huang DS. and X. Z. Mou "Molecular Imaging of Cancer with Nanoparticle-Based Theranostic Probes"; *Contrast Media & Molecular Imaging* Volume 2017, Article ID 1026270, 11 pages <https://doi.org/10.1155/2017/1026270>.
6. Mody VV, Siwale R. "Application of Nanoparticles in Diagnostic Imaging *via* Ultrasonography"; *Internet Journal of Medical Update* 2011 January;6(1):8–15; <http://www.akspublication.com/ijmu>.
7. Liu J, Levine AL, Matton JS. Nanoparticles as image enhancing agents for ultrasonography. *Phys Med Biol*. 2006May;51(9):2179–89.
8. Devarakonda SB, Myers MR, Giridhar D, Dibaji SAR, Banerjee RK. Enhanced thermal effect using magnetic nano-particles during high-intensity focused ultrasound. *PLoS ONE*. Apr. 2017;12(4):e0175093. 10.1371/journal.pone.0175093.
9. Johnston HJ, Semmler-Behnke M, Brown DM, Kreyling W, Tran L, Stone V. Evaluating the uptake and intracellular fate of polystyrene nanoparticles by primary and hepatocyte cell lines in vitro. *Toxicol Appl Pharmacol* vol. Jan. 2010;242(1):66–78. 10.1016/j.taap.2009.09.015.
10. Ekkapongpisit M, Giovia A, Follo C, Caputo G, Isidoro C. Biocompatibility, endocytosis, and intracellular trafficking of mesoporous silica and polystyrene nanoparticles in ovarian cancer cells:

- effects of size and surface charge groups. *Int J Nanomedicine* vol. Jul. 2012;7:4147–58. 10.2147/IJN.S33803.
11. Wang FJ, et al. Time resolved study of cell death mechanisms induced by amine-modified polystyrene nanoparticles. *Nanoscale*. Oct. 2013;5:10868–76. 10.1039/c3nr03249c.
  12. Firdessa R, Oelschlaeger TA, Moll H. Identification of multiple cellular uptake pathways of polystyrene nanoparticles and factors affecting the uptake: Relevance for drug delivery systems. *Eur J Cell Biol*. 2014;93:323–37. 10.1016/j.ejcb.2014.08.001., “”, , Aug-Sep.
  13. Monti DM, et al. Biocompatibility, uptake and endocytosis pathways of polystyrene nanoparticles in primary human renal epithelial cells. *J Biotechnol* vol. Jan. 2015;193:3–10. 10.1016/j.jbiotec.2014.11.004.
  14. Fiorentino I, et al. Energy independent uptake and release of polystyrene nanoparticles in primary mammalian cell cultures. *Exp Cell Res* vol. Jan. 2015;330(2):240–7. 10.1016/j.yexcr.2014.09.017.
  15. 10.1039/c4nr06849a  
Forte M, et al., “Polystyrene nanoparticles internalization in human gastric adenocarcinoma cells,” *Toxicol. In Vitro* vol. 31, pp. 126–136, Mar. 2016, and bio-reactivity of polystyrene nanoparticles is affected by surface modifications, ageing and LPS adsorption: in vitro studies on neural tissue cells,” *Nanoscale* vol. 7, pp. 4199–4210, Mar. 2015, 10.1039/c4nr06849a.
  16. 10.1007/s11051-014-2814-3  
Cabeza L, et al., “Polystyrene nanoparticles facilitate the internalization of impermeable biomolecules in non-tumour and tumour cells from colon epithelium,” *J. Nanopart. Res.* vol. 17, no. 1, art. 37, Jan. 2015, 10.1007/s11051-014-2814-3.
  17. 10.1016/j.bbamcr.2015.07.004  
Deville S, et al., “Intracellular dynamics and fate of polystyrene nanoparticles in A549 Lung epithelial cells monitored by image (cross-) correlation spectroscopy and single particle tracking,” *BBA-Mol. Cell Res.* vol. 1853, no. 10, pt. A, pp. 2411–2419, Oct. 2015, 10.1016/j.bbamcr.2015.07.004.
  18. 10.1080/01457632.2013.776877  
Wen D, “Nanoparticle-related heat transfer phenomenon and its application in biomedical fields. *Heat Transf. Eng.*, vol. 34, art. 14, pp. 1171–1179, Feb. 2013, 10.1080/01457632.2013.776877.
  19. Sviridov AP, Andreev VG, Ivanova EM, Osminkina LA, Tamarov KP, Timoshenko VY. “Porous silicon nanoparticles as sensitizers for ultrasonic hyperthermia,” *Appl Phys Lett*, 103, no. 19, art. 193110, Nov. 2013, 10.1063/1.4829148.
  20. 10.1115/1.4027340  
Dibaji SAR, Al-Rjoub MF, Myers MR, Banerjee RK, “Enhanced Heat Transfer and Thermal Dose Using Magnetic Nanoparticles During HIFU Thermal Ablation-An In-Vitro Study,” *J. Nanotechnol. Eng. Med.*, vol. 4, no. 4, art. 040902, Apr. 2014, 10.1115/1.4027340.
  21. Beik J, Abed Z, Shakeri-Zadeh A, Nourbakhsh M, Shiran MB. Evaluation of the sonosensitizing properties of nano-graphene oxide in comparison with iron oxide and gold nanoparticles. *Phys E*. Jul. 2016;81:308–14. 10.1016/j.physe.2016.03.023.

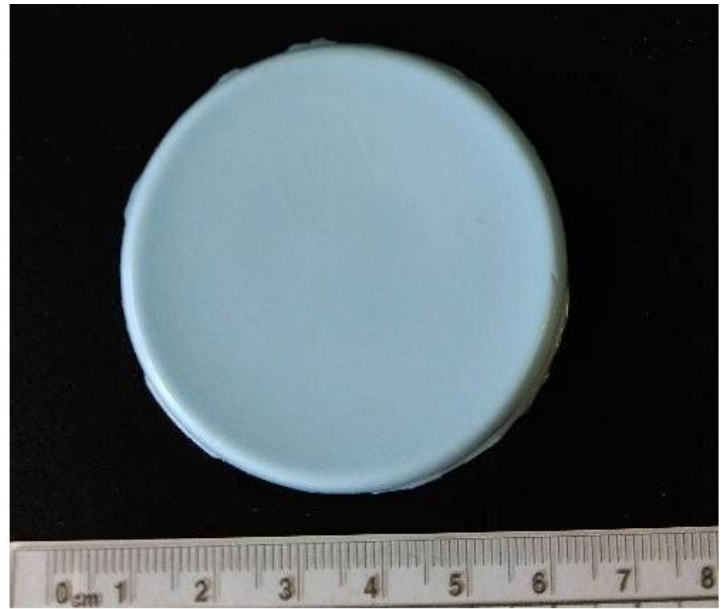
22. Waterman FM, Leeper JB. Temperature artifacts produced by thermocouples used in conjunction with 1 and 3 MHz ultrasound. *Int J Hyperthermia*. 1990;6(2):383–99. 10.3109/02656739009141146.
23. 10.1063/1.4955130  
Józefczak A, et al., “Magnetic nanoparticles for enhancing the effectiveness of ultrasonic hyperthermia,” *Appl. Phys. Lett.*, vol. 108, art. 263701, Jun. 2016, 10.1063/1.4955130.
24. Culjat MO, Goldenberg D, Tewari P, Singh RS. A Review of Tissue Substitutes for Ultrasound Imaging. *Ultrasound Med Biol*. Jun. 2010;36:6, pp. 861–73. 10.1016/j.ultrasmedbio.2010.02.012., “”, , no.
25. Madsen E, Frank GR, Dong F. “Liquid or Solid Ultrasonically Tissue- Mimicking Materials with Very Low Scatter,” *Ultrasound Med Biol.*, 24, 4, 535–42, May 1998, 10.1016/S0301-5629(98)00013 – 1.
26. Treece GM, Gee AH, Prager RW, Cash CJC, Berman LH. High-definition freehand 3-D ultrasound. *Ultrasound Med Biol*. Apr. 2003;29(4):529–46. 10.1016/S0301-5629(02)00735-4.
27. Bader KB, Crowe MJ, Raymond JL, Holland CK. Effect of Frequency-Dependent Attenuation on Predicted Histotripsy Waveforms in Tissue-Mimicking Phantoms. *Ultrasound Med Biol*. Jul. 2016;42(7):1701–5. 10.1016/j.ultrasmedbio.2016.02.010.
28. 10.1016/j.ultras.2016.10.014  
Papadopoulos N, Menikou G, Yiannakou M, Yiallouras C, Ioannides K, Damianou C, “Evaluation of a small flat rectangular therapeutic ultrasonic transducer intended for intravascular use,” *Ultrasonics* vol. 74, pp. 196–203, Feb. 2017, 10.1016/j.ultras.2016.10.014.
29. 10.1016/S0301-5629(97)00109-9  
Martin K, Fernandez R, “A Thermal Beam-shape Phantom for Ultrasound Physiotherapy Transducers,” *Ultrasound Med. Biol.*, vol 23, no. 8, pp. 1267–1274, 1997, 10.1016/S0301-5629(97)00109-9.
30. Dabbagh A, Abdullah BJJ, Kasim NHA, Ramasindarum C. Reusable heat-sensitive phantom for precise estimation of thermal profile in hyperthermia application. *Int J Hyperthermia*. 2014;30(1):66–74. 10.3109/02656736.2013.854930.
31. Negussie AH, et al. Thermochromic tissue-mimicking phantom for optimization of thermal tumour ablation. *Int J Hyperthermia*. Apr. 2016;32(3):239–43. 10.3109/02656736.2016.1145745.
32. Mikhail AS, Negussie AY, Graham C, Mathew M, Wood BJ, Partanen A. Evaluation of a tissue-mimicking thermochromic phantom for radiofrequency ablation. *Med Phys*. Jul. 2016;43(7):4304–11. 10.1118/1.4953394.
33. McDonald M, Lochhead S, Chopra R, Bronskill MJ, “Multi- modality tissue-mimicking phantom for thermal therapy,” *Phys. Med. Biol.*, vol. 49, no. 13, pp. 2767–2778, Jul. 2004.
34. Costa RM, Alvarenga AV, Costa-Felix RPB, Omena TP, von Krüger MA, Pereira WCA. Thermochromic Phantom and Measurement Protocol for Qualitative Analysis of Ultrasound Physiotherapy Systems. *Ultrasound Med Biol* vol. Jan. 2016;42(1):299–307. 10.1016/j.ultrasmedbio.2015.08.017.
35. Iwahashi T, et al., “Visualization of Temperature Distribution around Focal Area and Near Fields of High Intensity Focused Ultrasound Using
36. a 3D Measurement System,”. *Adv Biomed Eng* vol. Feb. 2018;7:1–7. 10.14326/abe.7.1.

37. Kim YT, Ma D, Sim JK, Kim SH. Simultaneous Evaluation of Thermal and Non-Thermal Effects of High-Intensity Focused Ultrasound on a Tissue-Mimicking Phantom. *Ultrasound Med Biol* vol. Aug. 2018;44(8):1799–809. 10.1016/j.ultrasmedbio.2018.03.024.
38. Anaheim. Sonicator 740 Instruction Manual. CA: Mettler Electronics Corp; 2013. p. 35.
39. Urick RJ. The Absorption of Sound in Suspensions of Irregular Particles. *J Acoust Soc Am* vol. May 1948;20(3):283–9. 10.1121/1.1906373.

## Figures



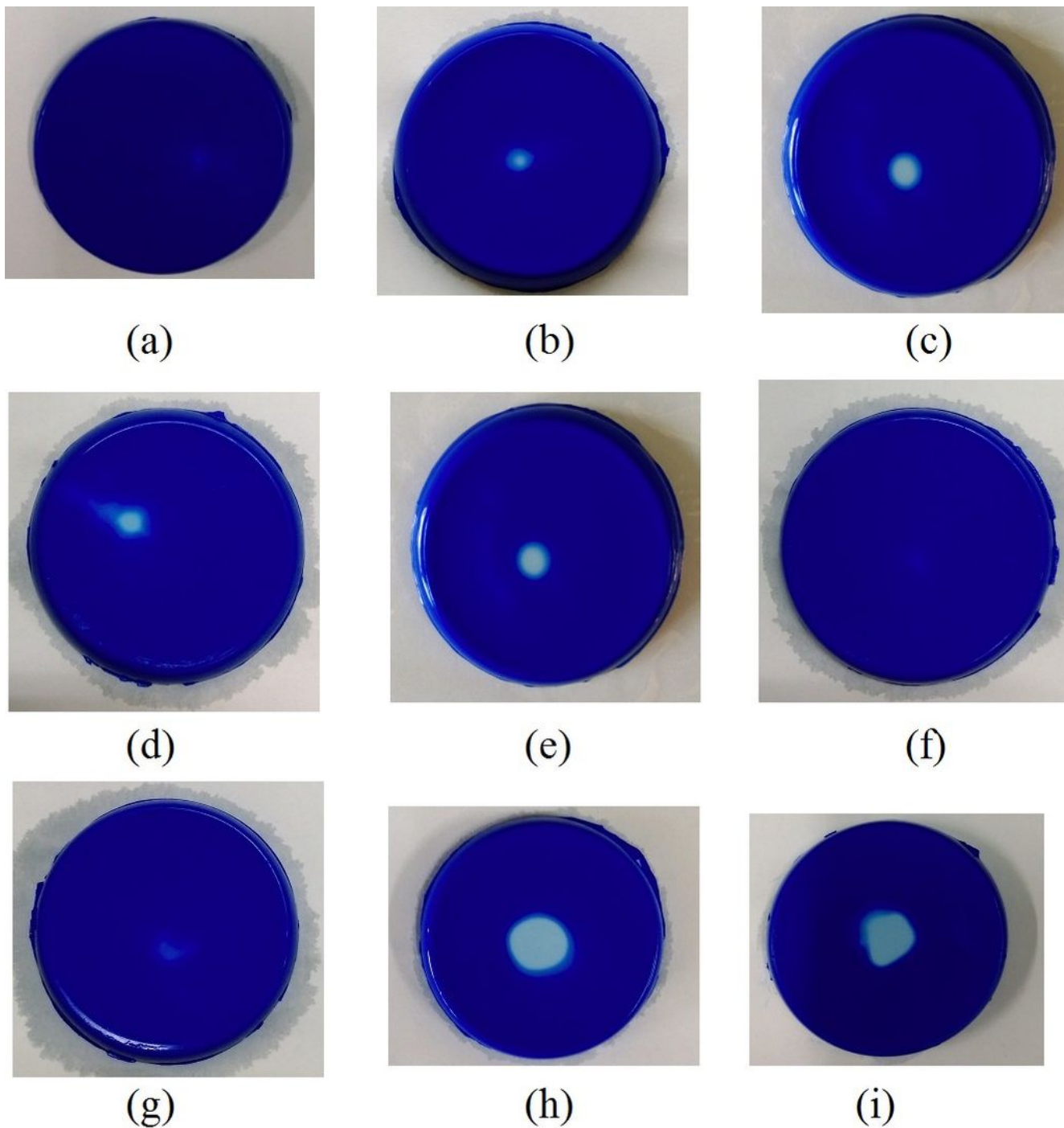
(a)



(b)

**Figure 1**

Agarose-based tissue mimicking gel (a) before and (b) after heating to 54 °C. The color change is irreversible such that reversion to room temperature of the white gel does not change its color back to blue.



—  
1 cm

**Figure 2**

Representative post ultrasound exposure gels. The gels are as follows: (a) control gel with no embedded nanoparticles, (b-e) gels containing 52.4 nm nanoparticles, with respectively  $3.3 \times 10^9$ ,  $6.6 \times 10^9$ ,  $3.3 \times 10^{12}$ , and  $6.6 \times 10^{12}$  particles each, and (f-i) gels containing 204.3 nm nanoparticles, with respectively  $5.6 \times 10^7$ ,  $1.1 \times 10^8$ ,  $5.6 \times 10^{10}$ , and  $1.1 \times 10^{11}$  particles each. Particle presence in sufficient numbers caused additional increases in temperature, which resulted in white areas to appear.

# Heated area comparison

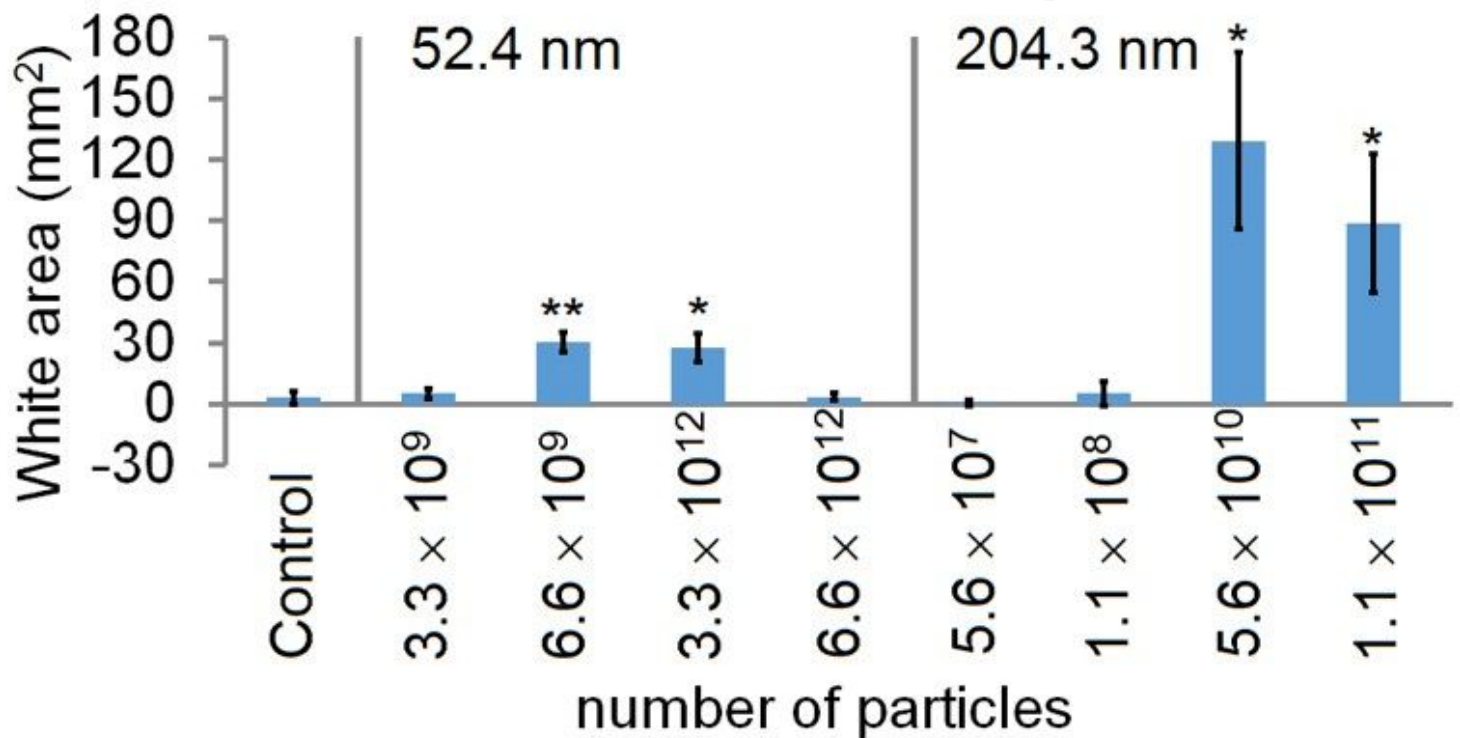
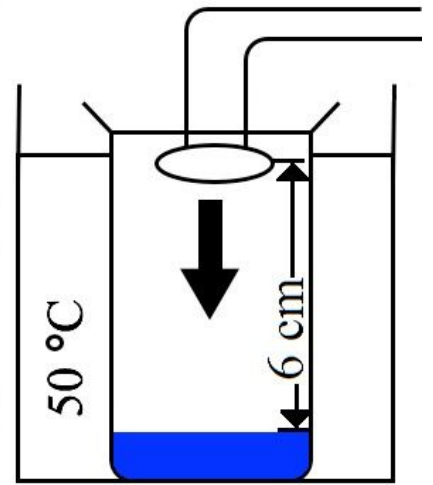


Figure 3

Comparison of heated areas. Ultrasonic exposure caused areas subjected to additional heating to become white. White areas were different depending on the number and size of embedded particles. Comparison of areas of experimental samples containing particles with those of non-particle bearing controls indicates that certain numbers of present particles cause larger areas to become heated. Error bars denote  $\pm 1$  standard deviation. Asterisks \* and \*\* respectively denote significant differences ( $0.01 < p \leq 0.05$ ) and ( $p \leq 0.01$ ). There were three gels examined ( $n = 3$ ) for every case.



(a)



(b)

#### Figure 4

Experimental setup (a) photograph and (b) schematic. A beaker containing gel material at its bottom is placed within an ultrasonic cleaner serving as a controlled-temperature water bath. The water bath temperature is set to 50 °C. An ultrasound transducer is placed above the beaker. Water bath levels covered the majority of the beaker. Water within the beaker was used as a coupling agent between the transducer and gel. The distance between the transducer face and gel surface was 6 cm.